Biochemical and Biophysical Research Communications 453 (2014) 69–74

Contents lists available at ScienceDirect

Biochemical and Biophysical Research Communications

journal homepage: www.elsevier.com/locate/ybbrc

Mutational definition of binding requirements of an hnRNP-like protein in *Arabidopsis* using fluorescence correlation spectroscopy

Verena Leder [a,b], Martina Lummer [a], Kathrin Tegeler [a,b], Fabian Humpert [b], Martin Lewinski [a], Mark Schüttpelz [b], Dorothee Staiger [a,*]

[a] Molecular Cell Physiology, Faculty of Biology, Bielefeld University, Germany
[b] Biomolecular Photonics, Faculty of Physics, Bielefeld University, Germany

ARTICLE INFO

Article history:
Received 2 September 2014
Available online 22 September 2014

Keywords:
RNA–protein-interaction
Fluorescence correlation spectroscopy
RNA-binding protein

ABSTRACT

Arabidopsis thaliana glycine-rich RNA binding protein 7 (*At*GRP7) is part of a negative feedback loop through which it regulates alternative splicing and steady-state abundance of its pre-mRNA. Here we use fluorescence correlation spectroscopy to investigate the requirements for *At*GRP7 binding to its intron using fluorescently-labelled synthetic oligonucleotides. By systematically introducing point mutations we identify three nucleotides that lead to an increased K_d value when mutated and thus are critical for *At*GRP7 binding. Simultaneous mutation of all three residues abrogates binding. The paralogue *At*GRP8 binds to an overlapping motif but with a different sequence preference, in line with overlapping but not identical functions of this protein pair. Truncation of the glycine-rich domain reduces the binding affinity of *At*GRP7, showing for the first time that the glycine-rich stretch of a plant hnRNP-like protein contributes to binding. Mutation of the conserved R^{49} that is crucial for *At*GRP7 function in pathogen defence and splicing abolishes binding.

1. Introduction

Heterogeneous nuclear ribonucleoproteins (hnRNPs) associate with nascent pre-mRNAs and mediate many steps in RNA processing. They possess one or more RNA-binding domains mostly of the RNA recognition motif (RRM) type and glycine-rich domains. The RRM is one of the most abundant protein domains with consensus motifs RNP-1 and RNP-2 that contact the RNA targets by hydrophobic interactions of conserved aromatic amino acid side chains [1].

In *Arabidopsis thaliana*, *At*GRP7 and *At*GRP8 are hnRNP-like proteins with an N-terminal RRM and a glycine-rich C-terminus [2]. The glycine-rich stretch harbours an M9 domain involved in nuclear import but otherwise its function is not clear [3–5]. *At*GRP7 and *At*GRP8 are regulators of alternative splicing and processing of a suite of microRNA precursors [6,7]. Both genes contain a single intron between RNP2 and RNP1 (Suppl. Fig. 1A). In transgenic plants that constitutively over-express *At*GRP7 an alternative splice form is generated that retains part of the intron with a premature termination codon and is rapidly degraded. *At*GRP7 protein binds to the *AtGRP7* 3′untranslated region (UTR) and intron *in vitro*, and *At*GRP7 is able to bind to its pre-mRNA *in vivo* [6,8]. Thus, the change in alternative splicing in response to elevated *At*GRP7 levels is a consequence of *At*GRP7 binding to its pre-mRNA [9,10]. Because alternative splicing of the *AtGRP7* pre-mRNA still occurs when the 3′UTR is replaced by a heterologous 3′UTR (unpublished), binding to the intron is likely to control the splice site choice.

We have previously adapted fluorescence correlation spectroscopy (FCS) to study RNA–protein-interaction at the single-molecule level [11]. FCS determines changes in diffusion constants upon ligand binding by analyzing fluctuations in signals from fluorescent molecules while passing the detection volume [12,13]. This relies on a fluorescent binding substrate whose diffusion constant and, hence, diffusion time through the detection volume changes upon binding to a non-fluorescent partner. Using fluorescently-labelled oligonucleotides and recombinant *At*GRP7 we have defined a minimal binding sequence within the *At*GRP7 3′UTR region [11]. Notably, this target site was used in an NMR study to resolve the structural basis of nucleic acid binding of a homologous glycine-rich RNA-binding protein, *Nt*GR-RBP1, from tobacco [14].

Here we perform a detailed mutational analysis of the sequence requirements for *At*GRP7 binding to its own intron. We find that the relative increase in diffusion time is a fast and reliable method

* Corresponding author. Address: Bielefeld University, 33501 Bielefeld, Germany. Fax: +49 521 1066410.
E-mail address: dorothee.staiger@uni-bielefeld.de (D. Staiger).

http://dx.doi.org/10.1016/j.bbrc.2014.09.056
0006-291X/

to screen a large number of point-mutated oligonucleotides. We identify three nucleotides critical for *At*GRP7 binding. *At*GRP8 binds to an overlapping motif but with a different sequence requirement. Truncation of the glycine-rich domain reduces the binding affinity of *At*GRP7, and mutation of the conserved R^{49} in RNP1 abolishes binding altogether.

2. Materials and methods

2.1. Recombinant proteins

The glutathione S-transferase (GST) fusion proteins GST-*At*GRP7, GST-*At*GRP7-R^{49}Q with R^{49} mutated, and GST-*At*GRP8 have been described [15,16]. A truncated *At*GRP7 lacking amino acids 128 to 176, GST-*At*GRP7 ΔGly, was generated by PCR (Suppl. Fig. 1B). Recombinant proteins were purified from *Escherichia coli* as described [9]. *At*GRP7 or *At*GRP8 moieties were released by on-column cleavage with PreScission® protease (GE Healthcare). The protein solution was concentrated using Centricon filter devices (Millipore).

2.2. Fluorescence correlation spectroscopy

FCS was performed on a custom-made confocal fluorescence microscope consisting of a standard inverse fluorescence microscope equipped with a HeNe laser, emitting at 632.8 nm, as excitation source and a pinhole of 100 μm. The collimated laser beam was coupled into an oil-immersion objective (x60, NA 1.35, Zeiss) by a dichroic beam-splitter (645DLRP, Omega Optical, Brattleboro, VT). The average laser power was adjusted to 0.5 mW before entering the aperture, to avoid population of the triplet states of the fluorophores as performed for MR121 which is structurally identical to Atto655 [17,18]. The fluorescence signal was collected by the same objective, filtered by a band-pass filter (700RDF75, Omega Optical), and imaged onto the active area of two single-photon avalanche photodiodes (APDs) (SPCM-AQR-14, PerkinElmer), sharing the fluorescence signal by a cubic nonpolarizing beamsplitter (Qioptiq). Using a real-time photon correlator (DPC-230, Becker & Hickl) the signals of the two APDs were recorded and cross-correlated (9 cycles per measurement, 100 s correlation time for each cycle). The application of two APDs at cross-correlation setting circumvents dead-time and afterpulsing effects.

Synthetic oligonucleotides with Atto655 (absorption maximum 663 nm, fluorescence emission maximum 684 nm) at the 3′end were diluted to 0.1 nM in phosphate-buffered saline, pH 7.4, 0.05% Tween-20. FCS measurements were carried out in 70 μl solution (63 μl oligonucleotide, 7 μl protein) enclosed by a recessed slide and a cover slip.

The correlation curves were analyzed assuming a simplified 2-dimensional diffusion model with a stretched-exponential term resembling the quenching dynamics of the dye [19]:

$$G(\tau) = \frac{1}{N} \cdot \frac{1}{1+\frac{\tau}{\tau_D}} \cdot \left(1 + A \cdot e^{-(k\tau)^{\beta}}\right) \quad (1)$$

where N is the number of molecules in the detection volume and τ_D the characteristic diffusion time through the detection volume. Quenching of the dye is modelled using a stretched-exponential term with amplitude A, rate constant k and stretch parameter β [11]. A stretched-exponential form is needed because of the contribution of multiple overlapping relaxation kinetics [17], assuming that the kinetics are independent so that superposition can be used to calculate the entire resultant kinetics. Eq. (1) is fit to the experimental data using the Levenberg–Marquardt least squares curve fitting algorithm to obtain the characteristic diffusion time τ_D.

2.3. Determination of the change in diffusion time and the dissociation constant K_d

The increase in diffusion time upon addition of a constant protein concentration to the labelled oligonucleotide is used to rapidly screen a large number of oligonucleotides. The relative increase in the diffusion time is

$$\Delta\tau_D = \frac{\tau_D^+}{\tau_D^-} - 1 \quad (2)$$

where τ_D^+ is the diffusion time in the presence of the protein and τ_D^- is the diffusion time of the oligonucleotide only. Unless otherwise stated, we used a 10^{-6} M protein concentration, which is expected to yield diffusion times in the saturated upper plateau.

The dissociation constant K_d is determined by varying the protein concentration from 10^{-9} M to 10^{-5} M and plotting τ_D versus the concentration on a semi-log scale, yielding a sigmoidal gradient with a lower and an upper plateau. The x-coordinate of the inflection point corresponds to the K_d value. For direct calculation of the K_d, the measured data was fitted by

$$y(x) = \frac{A_1 - A_2}{1 + \left(\frac{x}{K_d}\right)^p} + A_2 \quad (3)$$

where A_1 is the lower, A_2 is the upper plateau and p is a form factor describing the shape of the curve.

3. Results

3.1. FCS measurements of AtGRP7 binding to the intron of its pre-mRNA

To characterize *At*GRP7 binding to its intron, we performed an FCS measurement with the 31mer oligonucleotide 7-intron [15] (Supplementary Table S1). Because *At*GRP7 binds to single-stranded DNA and RNA with similar affinity we used DNA oligonucleotides to screen a large number of sequences [11]. Upon incubation of the oligonucleotide 7-intron with recombinant *At*GRP7 the diffusion time τ_D increased by $\Delta\tau_D = 53.53\% \pm 8.13\%$ relative to the free oligonucleotide, indicative of binding (Supplementary Fig. S2). The K_d for the interaction was 3.92×10^{-7} M ± 0.47×10^{-7} M (Table 1).

3.2. Delineation of the AtGRP7 binding site in the AtGRP7 intron

To narrow down the region responsible for binding, a series of short overlapping oligonucleotides spanning 7-intron were synthesized. The oligonucleotide 7-intron1 comprising the 5′terminal part of 7-intron showed a small relative increase in diffusion time of 13.6% ± 1.23% when *At*GRP7 protein was added (Supplementary Fig. S1). The oligonucleotides 7-intron3, 7-intron5, and 7-intron4 (spanning both 7-intron3 and 7-intron5) showed larger relative increases in diffusion time of 48.23% ± 2.42%, 31.64% ± 4.06%, and 54.82% ± 6.25%, respectively, upon addition of *At*GRP7 (Supplementary Fig. S2).

To determine whether *At*GRP7 binding to 7-intron3 and 7-intron5 indeed is weaker than binding to 7-intron4 we determined the K_d values by measuring the diffusion time τ_D for protein concentrations between 10^{-9} M and 10^{-5} M. The K_d values for 7-intron1 and 7-intron5 are one order of magnitude higher than that for 7-intron, suggesting that these regions only weakly interact with *At*GRP7 protein by themselves (Table 1). The K_d for 7-intron3 is in a range similar to the K_d of the 31mer 7-intron, indicating that the region of 7-intron3 is largely responsible for binding of *At*GRP7. The lowest K_d value was measured for 7-intron4. As 7-intron5 shows weaker interaction by itself, this

Table 1
Dissociation constants (K_d) of the interaction of *At*GRP7 with oligonucleotides derived from the *AtGRP7* intron.

Oligonucleotide	sequence	K_d (M)
7-intron	TTC AGT TTT GTT GGA TTG TTT TGC TGA TCT G	$3.92 \times 10^{-7} \pm 0.47 \times 10^{-7}$
7-intron1	TTC AGT TTT GTT	$1.75 \times 10^{-6} \pm 0.50 \times 10^{-6}$
7-intron3	TT GGA TTG TTT T	$4.52 \times 10^{-7} \pm 0.22 \times 10^{-7}$
7-intron4	TT GGA TTG TTT TGC TGA TCT G	$1.56 \times 10^{-7} \pm 0.09 \times 10^{-7}$
7-intron5	TT TGC TGA TCT G	$1.05 \times 10^{-6} \pm 0.02 \times 10^{-6}$
7-intron_mut4	TT GGA TCG TTT TGC TGA TCT G	n.d.
7-intron_mut6	TT GGA TTG CTT TGC TGA TCT G	$2.61 \times 10^{-6} \pm 0.35 \times 10^{-6}$
7-intron_mut13	TT GGA TTG TTT TGC TAA TCT G	$1.54 \times 10^{-6} \pm 0.33 \times 10^{-6}$

Mutated residues are highlighted in gray. n.d. not determined.

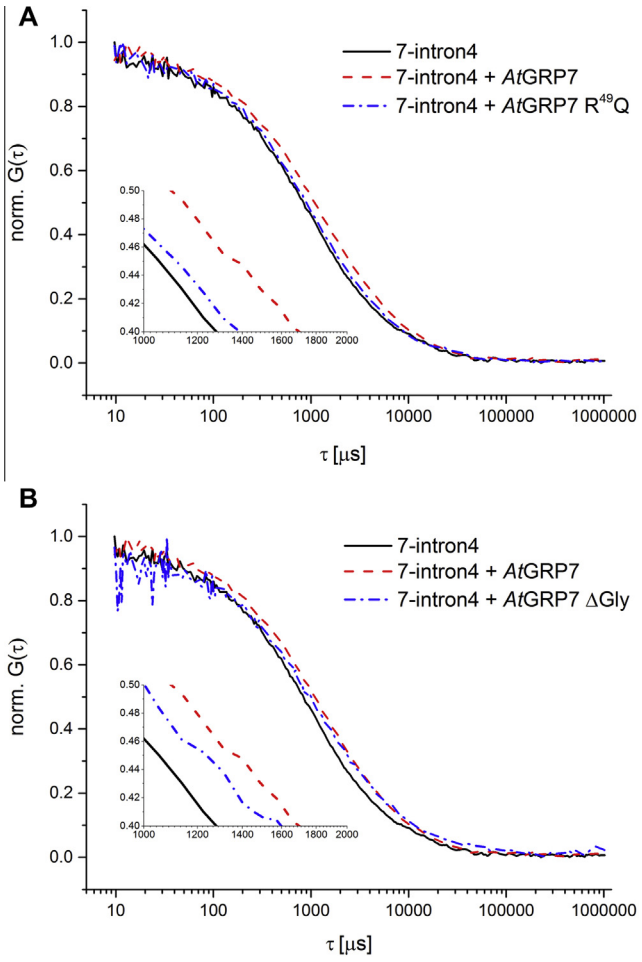

Fig. 1. Binding behavior of *At*GRP7 protein variants. (A) Correlation curves of free oligonucleotide 7-intron4, upon addition of *At*GRP7 wt and *At*GRP7 $R^{49}Q$ mutant protein, respectively. (B) Correlation curves of free oligonucleotide 7-intron4, upon addition of *At*GRP7 wt and *At*GRP7 ΔGly protein, respectively. The insets show an enlarged view on the range between 1000 and 2000 µs.

sequence may stabilize binding of *At*GRP7 to the region contained in 7-intron3 but is not sufficient to strongly bind *At*GRP7 by itself.

Furthermore, we tested the consequences of mutating the conserved R^{49} at the beginning of RNP1, as RNA contacts of the analogous arginine in human U1 small ribonucleoprotein A were identified in the crystal structure [20]. Addition of recombinant *At*GRP7 $R^{49}Q$ to 7-intron4 led to a negligible relative change in diffusion time of 2.21% ± 1.24% compared to the change caused by the authentic protein, indicating that R^{49} is crucial for the interaction (Fig. 1A).

3.3. Mutational analysis of AtGRP7 binding site requirements

To determine the contribution of individual nucleotides to the interaction with *At*GRP7 we systematically exchanged G and A, and T and C residues, respectively, in 7-intron4. In 7-intron_mut7/8 (further mut7/8), two Ts were mutated simultaneously. The increase in relative diffusion time upon addition of recombinant *At*GRP7 was similar to that for the 7-intron4 wild type (wt) sequence for mut1, mut3, mut5, mut7/8, mut14 and mut15, indicating that the exchange of the respective residues did not affect *At*GRP7 binding (Fig. 2). The changes in mut2, mut9, mut10, mut11, and mut12 led to a somewhat reduced increase in relative diffusion time. In contrast, mut4 (25.8% ± 2.27%) and mut13 (19.61% ± 2.31%) showed a much smaller increase in relative diffusion time upon addition of *At*GRP7 compared to 7-intron4, suggesting that mutation of residues 4 and 13 affected binding of *At*GRP7. The smallest relative increase in diffusion time and thus the strongest impairment of binding was observed for mut6 (11.50% ± 1.84%) (Fig. 2).

For the three mutant oligonucleotides which showed the strongest impairment of *At*GRP7 binding the K_d value was determined. For mut6 and mut13 the K_d values were one order of magnitude higher than for the wt sequence 7-intron4 (Table 1). For 7-intron_mut4 the low binding affinity precluded determination of the K_d value as the recombinant protein precipitated at the concentration needed to reach saturation. Thus, three nucleotides individually strongly reduce binding. An oligonucleotide with all three nucleotides exchanged simultaneously, 7-intron_mut4/6/13, showed a small increase in diffusion time of 11.5% ± 1.84% only (Fig. 2), indicating that the three nucleotides contribute greatly to *At*GRP7 binding.

3.4. Truncation of the AtGRP7 glycine-rich stretch reduces the binding affinity

*At*GRP7 resembles mammalian hnRNPs in consisting of an RRM and a region with a high glycine content and some interspersed arginine, tyrosine, and serine residues. To determine whether the glycine-rich stretch contributes to RNA binding we constructed a

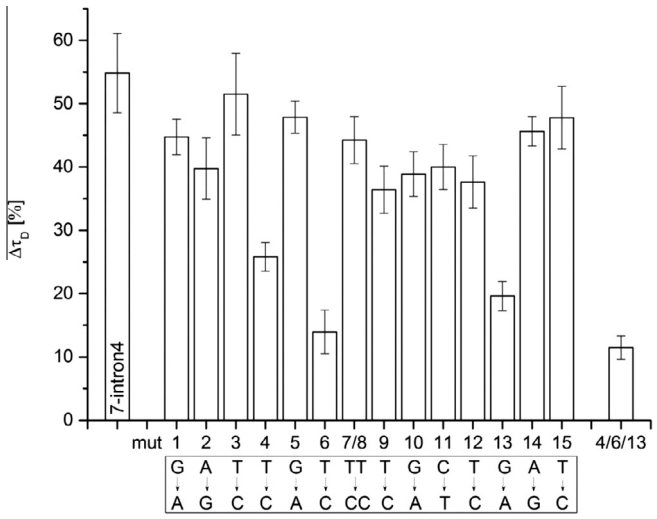

Fig. 2. Mutational analysis of *At*GRP7 interaction with 7-intron. The nucleotides mutated in each oligonucleotide and the relative change in diffusion time upon addition of *At*GRP7 protein are shown. Data are means of nine replicates ± s.d.

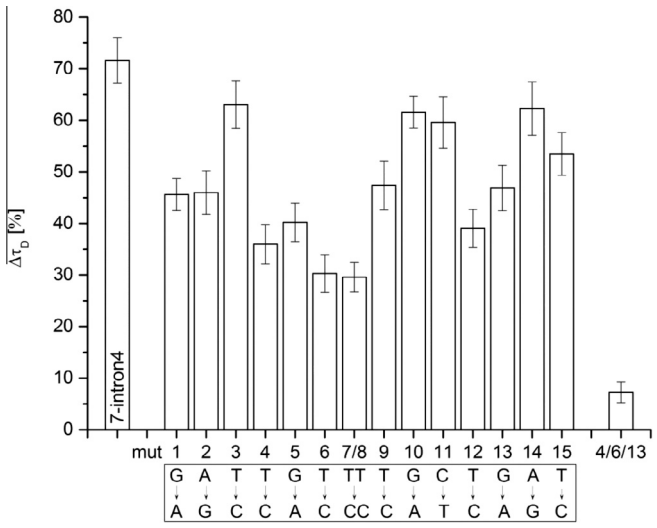

Fig. 3. Mutational analysis of *At*GRP8 interaction with 7-intron. The nucleotides mutated in each oligonucleotide and the relative change in diffusion time upon addition of *At*GRP8 protein are shown. Data are means of nine replicates ± s.d.

C-terminally truncated GST-*At*GRP7 variant retaining only part of the glycine stretch up to amino acid 127 (*At*GRP7 ΔGly). Upon addition of *At*GRP7 ΔGly to 7-intron4 an increase in diffusion time of only 26.6% ± 3.39% was measured compared to 54.82% ± 6.25% for the full length protein, suggesting reduced binding. Indeed, the K_d of *At*GRP7 ΔGly was increased to 7.78×10^{-6} M ± 0.1×10^{-6} M. The weaker interaction of *At*GRP7 ΔGly with 7-intron4 compared to wt *At*GRP7 protein suggests that the glycine-rich C-terminus of *At*GRP7 has a supportive role in RNA binding (Fig. 2B).

3.5. Identification of nucleotides critical for binding of AtGRP8 to the AtGRP7 intron

As *At*GRP8 also regulates alternative splicing of *AtGRP7*, it is conceivable that *At*GRP8 binds to an overlapping motif within the *AtGRP7* intron. Indeed, addition of *At*GRP8 protein led to a large change in relative diffusion time for 7-intron4 (Fig. 3) and similar K_d values were measured for 7-intron3, 7-intron4, and 7-intron5 (Table 2). Thus, *At*GRP8 appears to bind to these regions with a similar affinity, whereas *At*GRP7 shows a stronger interaction with 7-intron3 and 7-intron4. To determine the contribution of individual nucleotides to the interaction with *At*GRP8 we measured the relative diffusion times of the mutated 7-intron4 oligonucleotides (Fig. 3). Oligonucleotides mut3, mut10, mut11, mut14, and mut15 showed similar increases in relative diffusion time as 7-intron4, indicating that mutation of the corresponding nucleotides did not interfere with binding of *At*GRP8. For mut1, mut2, mut9, and mut13, an intermediate increase in relative diffusion time was observed, indicating that these mutations somewhat affected binding. A smaller increase in relative diffusion time was observed upon mutation of the T residues in mut4, mut5, mut6 (30.27% ± 3.60%), mut7/8 (29.58% ± 2.82%), and mut12, indicating that mutation of these T residues strongly impaired *At*GRP8 binding.

Notably, mutations located between nucleotides 4 and 8, and mutation of nucleotide 13, appear to have distinct effects on *At*GRP7 or *At*GRP8 binding. Mut4 shows a relative increase in diffusion time $\Delta\tau_D$ of 25.8% ± 2.27% for *At*GRP7 and of 35.95% ± 3.85% for *At*GRP8. The K_d for *At*GRP8 binding to mut4 was 3.39×10^{-7} M ± 1.08×10^{-7} M (Table 2) whereas the K_d for *At*GRP7 could not be determined. Thus, the exchange of T4 for C in mut4 impairs binding of *At*GRP7 much more than binding of *At*GRP8. The mut5 mutation affected binding of *At*GRP7 and *At*GRP8 to a similar degree. The K_d for *At*GRP8 binding to mut6 was 4.07×10^{-7} M ± 2.51×10^{-7} M whereas it was one order of magnitude higher (2.61×10^{-6} M ± 0.35×10^{-6} M) for *At*GRP7 (Table 1). Thus, the exchange of T6 for C in mut6 strongly impairs binding of *At*GRP7 but has little effect on *At*GRP8 binding. Mutation of the T residues 7 and 8 in mut7/8 moderately affected *At*GRP7 binding, but had the strongest effect of all mutations on *At*GRP8 binding. The triple mutant mut4/6/13 showed a change in relative diffusion time of 7.24% ± 2.01%, indicating that *At*GRP8 binding is abolished. The exchange of a G for an A in mut13 did not strongly impair *At*GRP8 binding although it led to an increase in K_d for *At*GRP7 by one order of magnitude. Thus, the loss of binding to mut4/6/13 likely is due to the mutations at positions 4 and 6.

4. Discussion

Ensemble measurements such as electrophoretic mobility shift assays provide information about protein-nucleic acid-interaction, but sufficient resolution to measure subtle differences in binding affinities is more difficult to obtain. We show that FCS is a fast and reliable method to define binding requirements and that the effects of single nucleotide mutations or site-specific mutation of a single amino acid can be resolved. To rapidly pre-screen combinations of oligonucleotide and protein variants, the increase in diffusion time of a fluorescently-labelled oligonucleotide upon addition of recombinant protein was measured. The determination of $\Delta\tau_D$ reduces the number of measurements and, hence, the use of substrate. Importantly, the relative increase in diffusion time does not depend on experimental parameters which allows for the direct comparison of diffusion times even if obtained with different setups with different focus dimensions and laser power settings. The dissociation constant K_d of the interaction is then determined for those protein-oligonucleotide pairs showing a large change in relative diffusion time.

Using oligonucleotides spanning the predicted *At*GRP7 binding site within the intron we identified the region 7-intron4 sufficient for high affinity binding of *At*GRP7. Using systematic mutagenesis we identified three nucleotides particularly critical for *At*GRP7 binding.

The paralogous protein *At*GRP8 binds to 7-intron4 with a similar affinity as *At*GRP7. In contrast to *At*GRP7 which only weakly

Table 2
Dissociation constants (K_d) of the interaction of *At*GRP8 with oligonucleotides derived from the *AtGRP7* intron.

Oligonucleotide	sequence	K_d (M)
7-intron	TTC AGT TTT GTT GGA TTG TTT TGC TGA TCT G	$1.39 \times 10^{-7} \pm 0.008 \times 10^{-7}$
7-intron1	TTC AGT TTT GTT	$5.24 \times 10^{-7} \pm 0.96 \times 10^{-7}$
7-intron3	TT GGA TTG TTT T	$2.14 \times 10^{-7} \pm 0.11 \times 10^{-7}$
7-intron4	TT GGA TTG TTT TGC TGA TCT G	$3.01 \times 10^{-7} \pm 0.73 \times 10^{-7}$
7-intron5	TT TGC TGA TCT G	$1.45 \times 10^{-7} \pm 0.16 \times 10^{-7}$
7-intron_mut4	TT GGA TCG TTT TGC TGA TCT G	$3.39 \times 10^{-7} \pm 1.08 \times 10^{-7}$
7-intron_mut6	TT GGA TTG CTT TGC TGA TCT G	$4.07 \times 10^{-7} \pm 2.51 \times 10^{-7}$
7-intron_mut13	TT GGA TTG TTT TGC TAA TCT G	n.d.

Mutated residues are highlighted in gray. n.d. not determined.

binds to 7-intron5, the 3′half of 7-intron4, *At*GRP8 binds to 7-intron3, 7-intron4, and 7-intron5 with a similar affinity. This may indicate that *At*GRP8 has more than one binding site.

Several mutations which did not strongly impair *At*GRP7 binding did not affect *At*GRP8 binding either. However, we also found distinct differences. Mut4 affected *At*GRP7 binding more strongly than *At*GRP8 binding. The exchange of T6 for C in mut6 strongly impaired binding of *At*GRP7 but had less effect on *At*GRP8 binding. Mutation of T7 and T8 in mut7/8 moderately affected *At*GRP7 binding, but had the strongest effect of all mutations on *At*GRP8 binding. The relative impact of the mutations at each position is summarized in Supplementary Fig. S3. The differences in binding affinities correspond to the notion that *At*GRP7 and *At*GRP8 share overlapping functions but are not entirely redundant. Upon loss of *AtGRP7* in *atgrp7-1* mutant plants, *At*GRP8 is up-regulated but nevertheless the mutant flowers later, is more sensitive to pathogens and shows aberrant splicing and levels of target transcripts [6,21–24].

*At*GRP7 is a simplified version of mammalian hnRNPs. Whereas it is well established that the RRM mediates the RNA-binding activity, the function of the glycine stretch in plant hnRNPs is largely unknown. *At*GRP7 complemented the cold-sensitivity of an *E. coli* mutant lacking cold-shock proteins through the RRM whereas the glycine stretch had no effect [25]. For *Nt*GR-RBP1, the glycine stretch has been shown to promote self-association and thereby enhance its chaperone activity [14]. So far the glycine stretch of *At*GRP7 is thought to harbour an M9-domain involved in nuclear trafficking [3,4]. Here we show that truncation of the glycine stretch from positions 176 to 127 reduced the *in vitro* binding activity. This assigns a previously unidentified role to the glycine stretch: It may have an accessory role in RNA binding as previously noted for the glycine stretch of the prototype hnRNP protein, mammalian hnRNP A1 [26]. RNA bandshift experiments have shown that the *At*GRP7 glycine stretch by itself does not bind to RNA (unpublished).

Furthermore, we show that mutation of the conserved R^{49} strongly interferes with the binding activity in line with the strong impairment of *in vivo* function upon mutation of R^{49} [6,15,27]. Notably, ADP-ribosylation of R^{49} by the *Pseudomonas syringae* type III effector HopU1 interferes with *At*GRP7 function in immunity [21,23,24].

Previous FCS studies with nucleic acids were performed on the dimerization of RNA molecules [28] and RNA dynamics was monitored by analyzing fluorophore binding RNA aptamers [29]. RNA–protein interaction was studied for the HIV Tat-responsive-element and a peptide derived from Tat using fluorescence cross-correlation spectroscopy [30]. In this case, both the synthetic peptide and synthetic oligonucleotides were labeled. We show that FCS is successfully adapted for rapid screening of a collection of fluorescently labeled oligonucleotides for binding to an unlabeled cognate protein. We reliably detected binding of a rather small molecule, i.e., the molecular weight of the bound partners is only 2–3 times compared to the weight of the fluorescently-labelled substrate molecule. Hence, FCS is not only applicable when a sufficient increase of the molecular weight is observed upon interaction of the partners to rapidly and quantitatively reveal information on molecular interactions at the single-molecule level.

Acknowledgment

This work was supported by the German Research Foundation [STA 653, SFB613].

Appendix A. Supplementary data

Supplementary data associated with this article can be found, in the online version, at http://dx.doi.org/10.1016/j.bbrc.2014.09.056.

References

[1] C. Maris, C. Dominguez, F.H. Allain, The RNA recognition motif, a plastic RNA-binding platform to regulate post-transcriptional gene expression, FEBS J. 272 (2005) 2118–2131.
[2] G. Sachetto-Martins, L.O. Franco, D.E. de Oliveira, Plant glycine-rich proteins: a family or just proteins with a common motif?, Biochim Biophys. Acta 1492 (2000) 1–14.
[3] A. Ziemienowicz, D. Haasen, D. Staiger, T. Merkle, *Arabidopsis* transportin1 is the nuclear import receptor for the circadian clock-regulated RNA-binding protein *At*GRP7, Plant Mol. Biol. 53 (2003) 201–212.
[4] M. Lummer, F. Humpert, C. Steuwe, M. Schüttpelz, M. Sauer, D. Staiger, Reversible photoswitchable DRONPA-s monitors nucleocytoplasmic transport of an RNA-binding protein in transgenic plants, Traffic 12 (2011) 693–702.
[5] H. Siomi, G. Dreyfuss, A nuclear localization domain in the hnRNP A1 protein, J. Cell Biol. 129 (1995) 551–560.
[6] C. Streitner, T. Köster, C.G. Simpson, P. Shaw, S. Danisman, J.W.S. Brown, D. Staiger, An hnRNP-like RNA-binding protein affects alternative splicing by in vivo interaction with target transcripts in *Arabidopsis thaliana*, Nucleic Acids Res. 40 (2012) 11240–11255.
[7] T. Köster, K. Meyer, C. Weinholdt, L.M. Smith, M. Lummer, C. Speth, I. Grosse, D. Weigel, D. Staiger, Regulation of pri-miRNA processing by the hnRNP-like protein AtGRP7 in *Arabidopsis*, Nucleic Acids Res. 24 (2014).
[8] D. Staiger, L. Zecca, D.A. Wieczorek Kirk, K. Apel, L. Eckstein, The circadian clock regulated RNA-binding protein AtGRP7 autoregulates its expression by

influencing alternative splicing of its own pre-mRNA, Plant J. 33 (2003) 361–371.
[9] J.C. Schöning, C. Streitner, I.M. Meyer, Y. Gao, D. Staiger, Reciprocal regulation of glycine-rich RNA-binding proteins via an interlocked feedback loop coupling alternative splicing to nonsense-mediated decay in *Arabidopsis*, Nucleic Acids Res. 36 (2008) 6977–6987.
[10] C. Schmal, P. Reimann, D. Staiger, A circadian clock-regulated toggle switch explains AtGRP7 and AtGRP8 oscillations in *Arabidopsis thaliana*, PLoS Comput. Biol. (2013).
[11] M. Schüttpelz, J.C. Schöning, S. Doose, H. Neuweiler, E. Peters, D. Staiger, M. Sauer, Changes of conformational dynamics of mRNA upon AtGRP7 binding studied by fluorescence correlation spectroscopy, J. Am. Chem. Soc. 130 (2008) 9507–9513.
[12] H. Neuweiler, M. Lollmann, S. Doose, M. Sauer, Dynamics of unfolded polypeptide chains in crowded environment studied by fluorescence correlation spectroscopy, J. Mol. Biol. 365 (2007) 856–869.
[13] E. Haustein, P. Schwille, Fluorescence correlation spectroscopy: novel variations of an established technique, Annu. Rev. Biophys. Biomol. Struct. 36 (2007) 151–169.
[14] F. Khan, M.A. Daniëls, G.E. Folkers, R. Boelens, S.M. Saqlan Naqvi, H.V. Ingen, Structural basis of nucleic acid binding by *Nicotiana tabacum* glycine-rich RNA-binding protein: implications for its RNA chaperone function, Nucleic Acids Res. 42 (2014) 8705–8718.
[15] J.C. Schöning, C. Streitner, D.R. Page, S. Hennig, K. Uchida, E. Wolf, M. Furuya, D. Staiger, Autoregulation of the circadian slave oscillator component *At*GRP7 and regulation of its targets is impaired by a single RNA recognition motif point mutation, Plant J. 52 (2007) 1119–1130.
[16] A. Fuhrmann, J.C. Schoening, D. Anselmetti, D. Staiger, R. Ros, Quantitative analysis of single-molecule RNA–protein interaction, Biophys. J. 96 (2009) 5030–5039.
[17] J. Kim, S.R. Doose, H. Neuweiler, M. Sauer, The initial step of DNA hairpin folding: a kinetic analysis using fluorescence correlation spectroscopy, Nucleic Acids Res. 34 (2006) 2516–2527.
[18] S. Doose, H. Neuweiler, M. Sauer, A close look at fluorescence quenching of organic dyes by tryptophan, ChemPhysChem 6 (2005) 2277–2285.
[19] S. Doose, H. Barsch, M. Sauer, Polymer properties of polythymine as revealed by translational diffusion, Biophys. J . 93 (2007) 1224–1234.
[20] K. Nagai, C. Oubridge, T.H. Jessen, J. Li, P.R. Evans, Crystal structure of the RNA-binding domain of the U1 small nuclear ribonucleoprotein A, Nature 348 (1990) 515–520.
[21] Z.Q. Fu, M. Guo, B.R. Jeong, F. Tian, T.E. Elthon, R.L. Cerny, D. Staiger, J.R. Alfano, A type III effector ADP-ribosylates RNA-binding proteins and quells plant immunity, Nature 447 (2007) 284–288.
[22] C. Streitner, S. Danisman, F. Wehrle, J.C. Schöning, J.R. Alfano, D. Staiger, The small glycine-rich RNA-binding protein *At*GRP7 promotes floral transition in *Arabidopsis thaliana*, Plant J. 56 (2008) 239–250.
[23] B.-R. Jeong, Y. Lin, A. Joe, M. Guo, C. Korneli, H. Yang, P. Wang, M. Yu, R.L. Cerny, D. Staiger, J.R. Alfano, Y. Xu, Structure function analysis of an ADP-ribosyltransferase type III effector and its RNA-binding target in plant immunity, J. Biol. Chem. 286 (2011) 43272–43281.
[24] V. Nicaise, A. Joe, B. Jeong, C. Korneli, F. Boutrot, I. Wested, D. Staiger, J.R. Alfano, C. Zipfel, Pseudomonas HopU1 affects interaction of plant immune receptor mRNAs to the RNA-binding protein GRP7, EMBO J. 32 (2013) 701–712.
[25] J.S. Kim, S.J. Park, K.J. Kwak, Y.O. Kim, J.Y. Kim, J. Song, B. Jang, C.H. Jung, H. Kang, Cold shock domain proteins and glycine-rich RNA-binding proteins from *Arabidopsis thaliana* can promote the cold adaptation process in *Escherichia coli*, Nucleic Acids Res. 35 (2006) 506–516.
[26] F. Cobianchi, C. Calvio, M. Stoppini, M. Buvoli, S. Riva, Phosphorylation of human hnRNP protein A1 abrogates in vitro strand annealing activity, Nucleic Acids Res. 21 (1993) 949–955.
[27] C. Streitner, L. Hennig, C. Korneli, D. Staiger, Global transcript profiling of transgenic plants constitutively overexpressing the RNA-binding protein AtGRP7, BMC Plant Biol. 10 (2010) 221.
[28] A. Werner, P.V. Konarev, D.I. Svergun, U. Hahn, Characterization of a fluorophore binding RNA aptamer by fluorescence correlation spectroscopy and small angle X-ray scattering, Anal. Biochem. 389 (2009) 52–62.
[29] A. Werner, V. Skakun, C. Meyer, U. Hahn, RNA dimerization monitored by fluorescence correlation spectroscopy, Eur. Biophys. J. 40 (2011) 907–921.
[30] C.K. Nandi, P.P. Parui, B. Brutschy, U. Scheffer, M. Göbel, Fluorescence correlation spectroscopy at single molecule level on the Tat–TAR complex and its inhibitors, Biopolymers 89 (2008) 17–25.